

Linear simulation of ion temperature gradient driven instabilities in W7-X and LHD stellarators using GTC

Hongyu Wang,¹ Zhihong Lin,^{1,2} Ihor Holod,² Jian Bao,^{1,2} Lei Shi,² and Sam Taimourzadeh²

¹*Fusion Simulation Center, Peking University, Beijing 100871, China*

²*Department of Physics and Astronomy, University of California, Irvine, California 92697, USA*

Abstract

The global gyrokinetic toroidal code (GTC) has been recently upgraded to do simulations in non-axisymmetric equilibrium configuration, such as stellarators. Linear simulation of ion temperature gradient (ITG) driven instabilities has been done in Wendelstein7-X (W7-X) and Large Helical Device (LHD) stellarators using GTC. Several results are discussed to study characteristics of ITG in stellarators, including toroidal grids convergence, nmodes number convergence, poloidal and parallel spectrums, and electrostatic potential mode structure on flux surface.

I. INTRODUCTION

After stellarators being designed in 1950s, several concepts in magnetic confinement devices are first presented in stellarators [reference1] and recently increasing attentions have been put on magnetic confinement devices with symmetry-breaking effects [reference2]. The non-axisymmetric feature in toroidal direction of stellarator brings many unique physical phenomenons and possible method of nuclear fusion. At the same time, considering the common properties of tokamak and stellarator, like new classical transport and Alfvén eigenmodes, research achievements of plasma physics in stellarators also help deeper understanding of tokamaks [reference3]. W7-X, the biggest stellarator in the world currently, first produced helium plasma in December 2015, and LHD firstly produced plasma in 1998 and nowadays plasma confinement properties of LHD are comparable to world's fusion devices. As stellarator is one kind of hopeful devices to make nuclear fusion come true, it is necessary to study characteristics of plasma physics in stellarators in both experiments and computer simulations.

Several efforts have been put into simulations on stellarators. EUTERPE, a global particle-in-cell code, has been used to study the effects of collisions on ITG in LHD [reference4] and radial electric fields effects on linear ITG in W7-X and LHD [reference5]. GENE has done nonlinear simulation of ITG turbulence in W7-X [reference6] and compared simulation results of microinstabilities and turbulence with EUTERPE [reference7]. Linear simulations of ITG instabilities have also been studied for both standard and inward-shifted LHD configurations using GKV code [reference8], and a upgraded code, GKV-X, has done linear simulations of ITG using precise magnetic configurations of LHD, and comparisons between linear simulation results of ITG using GKV-X and LHD experiments observations are also given[reference9].

Recently, the global gyrokinetic toroidal code (GTC) has been upgraded to use 3D equilibrium geometry and study plasma phenomenons in stellarators caused by non-axisymmetric equilibrium configurations. GTC is a global gyrokinetic particle-in-cell code [reference10], and a field-aligned magnetic coordinate (ψ, θ, ζ) is employed in GTC to represent magnetic fields and profiles of

equilibrium quantities. To build realistic magnetic configurations, Variational Moments Equilibrium Code (VMEC) [reference11] is used in GTC. In this article, ion temperature gradient (ITG) instabilities in W7-X and LHD are explored using GTC and the simulations are all done in full torus. Effects of parallel grids and different modes coupling in W7-X and LHD on growth rates and real frequencies are investigated. Electrostatic potential on flux surface and 3D mode structures are also presented to study common characteristics and differences of ITG in W7-X and LHD.

The remainder of this paper is as follows. The method to upgrade GTC and construct non-axisymmetric magnetic fields using VMEC is presented in Section II. In Section III, simulation results of ITG in W7-X are given. Parallel grids convergence and Nmode convergence are studied to explore unique features caused by field periods of W7-X in parallel direction. Electrostatic potential on flux surface is plotted in (θ, ζ) space and 3D space to show mode structure directly. In section IV, simulation results of ITG in LHD are presented. Considering different technical structures of LHD and W7-X, parallel grids convergence, Nmode convergence, and mode structures are also studied in LHD. Conclusion and discussion are provided in Section V.

II. CONSTRUCT NON-AXISYMMETRIC MAGNETIC FIELDS USING VMEC

Thanks to the collaboration between the GTC team at UCI and Spong at ORNL, GTC has recently been updated to treat 3D equilibria by interfacing with MHD equilibrium code VMEC. The equilibrium geometry and magnetic field data from VMEC is provided in the form of Fourier series coefficients B_{cn} , B_{sn} in ζ -expansion:

$$B(\psi, \theta, \zeta) = \sum_{n=1}^N \left[B_{cn}(\psi, \theta, n) \cos(n\theta + n\zeta) + B_{sn}(\psi, \theta, n) \sin(n\theta + n\zeta) \right] \quad (1)$$

where (ψ, θ, ζ) are normalized poloidal flux, poloidal angle, and toroidal angle, respectively, forming right-handed Boozer coordinate system. The magnetic field ζ -dependence needs to be taken into account in the particle dynamics, gyrokinetic equation, and in the electron continuity equation.

The data in the form of Eq. (1) are provided for the magnetic field strength B , and cylindrical coordinates $(X, Z, \Phi - \zeta)$ of points forming magnetic flux surfaces. Additionally, the flux functions representing poloidal $g(\psi)$ and toroidal $I(\psi)$ currents, effective minor radius $r(\psi)$, and magnetic safety factor $q(\psi)$, are provided. The data is presented on uniform grid in $\psi = [0 : \psi_w]$, and $\theta = [0 : 2\pi]$, with the number of grid points l_{sp} and l_{st} , respectively for all N toroidal modes.

To reduce the computational load and memory usage, the transformation of non-axisymmetric variables into spline function of ψ is chosen, with spline coefficients associated with particular grid point i being stored by processors with corresponding toroidal domain location value. Thus, each MPI keeps $27 * m_{grid}$ (m_{grid} is the total grid number) values of quadratic spline

coefficients, compared to $9 \times m_{grid}$ in axisymmetric case. The values of equilibrium quantities are

calculated as $B(\psi, \theta, \zeta) = \sum_{i=1}^{27} B_i dx_i$, where B_i are the spline coefficients; $dx_1 = 1$,

$$dx_2 = \Delta\psi, \quad dx_3 = \Delta\psi^2, \quad dx_{4-6} = dx_{1-3}\Delta\theta, \quad dx_{7-9} = dx_{1-3}\Delta\theta^2, \quad dx_{10-18} = dx_{1-9}\Delta\zeta,$$

$dx_{19-27} = dx_{1-9}\Delta\zeta^2$, and $\Delta\psi, \Delta\theta, \Delta\zeta$ are the distances from the nearest lower spline-grid points.

The 3D spline coefficients are found by consecutively constructing 1D spline for each coefficient of lower-dimension spline. In spline3d, for each toroidal grid point the expansion sum (1) is calculated and its value send to construct_spline2d, where for every θ -grid point the 1D spline in ψ -direction is constructed, and then for every ψ -grid point each of obtained 3 spline coefficients is spline-interpolated in θ -direction, giving 9 coefficients. After that, the 1D spline in ζ is constructed for each of 9 coefficients, giving 27 coefficients for every $m_{toroidal} \times m_{grid}$ grids. Finally, the spline-coefficients associated with particular ζ -grid point are passed to PEs having corresponding value of toroidal domain location.

III. SIMULATION OF ITG IN W7-X

In a stellarator, both device configuration and produced plasma are not axisymmetric in toroidal direction anymore, and the cross sections of stellarator change at different toroidal angles. Poloidal contours look the same only after rotating a stellarator at certain angles in toroidal direction. Field period, N_{fp} , is used to describe this non-axisymmetric feature in stellarators, and it gives the rotating toroidal angle needed to make the poloidal contours looking the same. For W7-X, field period is 5 and it means the same cross sections of W7-X will be found through a minimum angle

of 72° in toroidal direction. The 2D poloidal contours at $\zeta = \frac{0}{N_{fp}}, \frac{0.5\pi}{N_{fp}}, \frac{\pi}{N_{fp}}, \frac{1.5\pi}{N_{fp}}$ on

diagnosis flux surface of W7-X are given in FIG1.

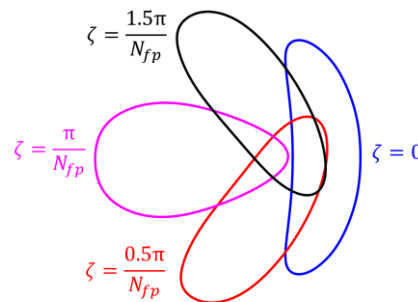


Figure 1. 2D poloidal contours of W7-X on diagnosis flux surface at $\zeta = 0$ (blue), $\zeta = 0.5\pi / N_{fp}$ (red), $\zeta = \pi / N_{fp}$ (magenta) and $\zeta = 1.5\pi / N_{fp}$ (black). N_{fp} is field period and $N_{fp} = 5$ in W7-X.

Rotational transform is used to present magnetic field line traveling angles in toroidal and poloidal

direction in stellarators and $\Delta\psi=1/q$, while q is safety factor in tokamaks. Ion temperature profile, in which ion temperature gradient η is 1, and rotational transform profile are given in FIG2(a). Simulation range of ψ is also marked out in FIG2, and diagnosis point is at $\psi=0.5$. Basic parameters used in simulations of W7-X are as follows: magnetic field on axis is 23600 Gauss, ion temperature at diagnosis point is 1000 eV, major radius is 561.79 cm, $k_\perp\rho_i=0.0089$, time step is 0.01 Cs/R0, and Cs/R0 is 2.43E-04. Growth rates and real frequencies of simulations in this section are normalized to Cs/R0. As introduced in Section I, Fourier series coefficients in ζ expansion are used to build 3D magnetic field in GTC. Harmonic series $n_{\text{tor}}(n)$ is an arithmetic progression with common difference of 5, so the first 4 harmonic Fourier series n_{tor} are 0, 5, 10, 15. The first 4 Fourier series coefficients $B_{cn}(\psi,1,1)$, $B_{cn}(\psi,1,2)$, $B_{cn}(\psi,1,3)$,

$B_{cn}(\psi,1,4)$ used to construct 3D magnetic field of W7-X are given in FIG2(b).

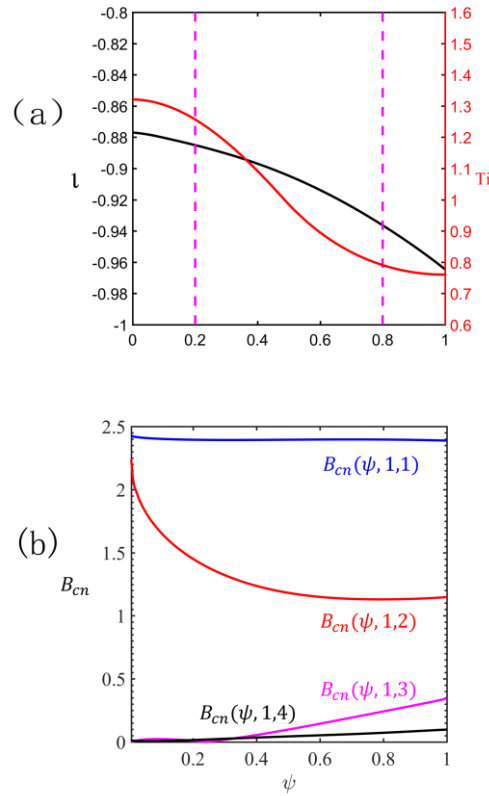


Figure 2. (a) Ion temperature (red) profile and rotational transform (black) profile. Simulation range is marked out by magenta lines: $\psi_{\text{inner}}=0.2$ and $\psi_{\text{outer}}=0.8$. (b) Fourier series coefficients of magnetic field of W7-X used in GTC, $B_{cn}(\psi,1,1)=0$ (blue), $B_{cn}(\psi,1,2)=5$ (red), $B_{cn}(\psi,1,3)=10$ (magenta), $B_{cn}(\psi,1,4)=15$ (black). Values of $B_{cn}(\psi,1,2)$, $B_{cn}(\psi,1,3)$, $B_{cn}(\psi,1,4)$ are multiplied by 10.

Considering non-axisymmetric equilibrium of W7-X, it is important to study parallel grids needed in simulations. Growth rates and real frequencies of $n_{\text{mode}}=185$, $m_{\text{mode}}=205$ when parallel grids $N_p=17, 33, 65$, and 97 are shown in FIG3. Parallel spectrums for different parallel grids are given in FIG4. According to growth rates, real frequencies and parallel spectrums, 65 parallel grids are needed to do full torus simulations in W7-X using GTC. As the coordinate of GTC is field-aligned, parallel grids needed are smaller to get convergence and it saves the computing resource greatly.

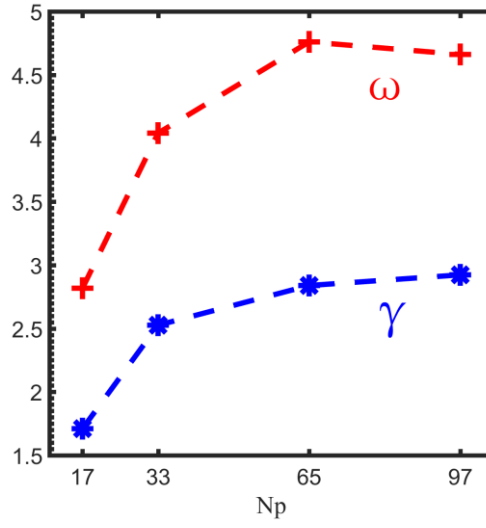


Figure 3. Growth rates (blue) and real frequencies (red) of parallel grids convergence.

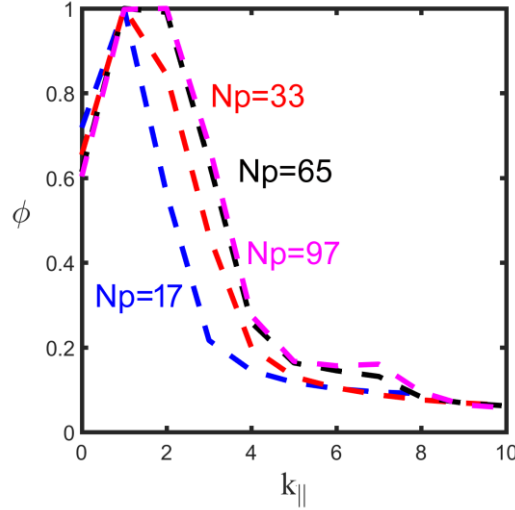


Figure 4. Parallel spectrums of different parallel grids.

In GTC, after solving fields, a filtering step is put before gathering particles, so nmodes number. Nmode, can be set by choosing whether doing filtering. To study different modes coupling effects in W7-X, convergence of nmodes number also should be done. In simulations, one nmode, 3 nmodes, 7 nmodes and all nmodes are kept to study convergence of nmodes number convergence. When keeping only one nmode, all nmodes except nmodes=185 are filtered out. As filed period of W7-X is 5, nmodes=180, 185, 190 are kept when Nmode=3, and nmodes=170, 175, 180, 185, 190, 195, 200 are kept when Nmode=7. When keeping all nmodes in simulation, filtering step is omitted. Growth rates and real frequencies of nmode=185, mmode=205 are shown in FIG5.

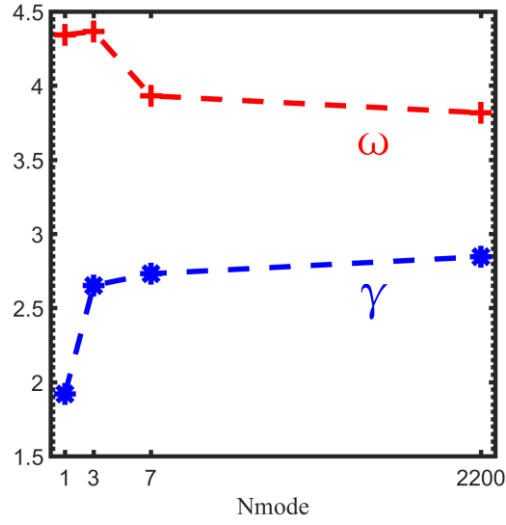


Figure 5. Growth rates (blue) and real frequencies (red) of Nmode convergence.

Growth rates and real frequencies of $n_{mode}=185$ at different ion temperature gradients η are given in FIG6, and η is defined as $\eta = -\frac{d \ln T_i}{d \psi_{tor}}$. In these cases, 3 nmodes are kept in simulations. These growth rates and real frequencies show good linearity with ion temperature gradient and are compared with simulation results of EUTERPE.

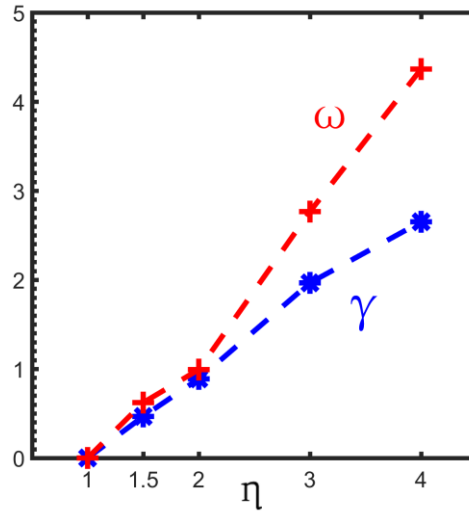


Figure 6. Growth rates (blue) and real frequencies (red) of $n_{mode}=185$ and $m_{mode}=205$ when keeping 3 nmodes in simulation.

Fast Fourier Transform Algorithm is used to calculate poloidal spectrum on flux surface. An average poloidal spectrum of diagnosis flux surface and other 10 flux surfaces, which are closet to diagnosis flux surface, is given in FIG7. Peak value of poloidal spectrum appears at around $m_{mode}=400$.

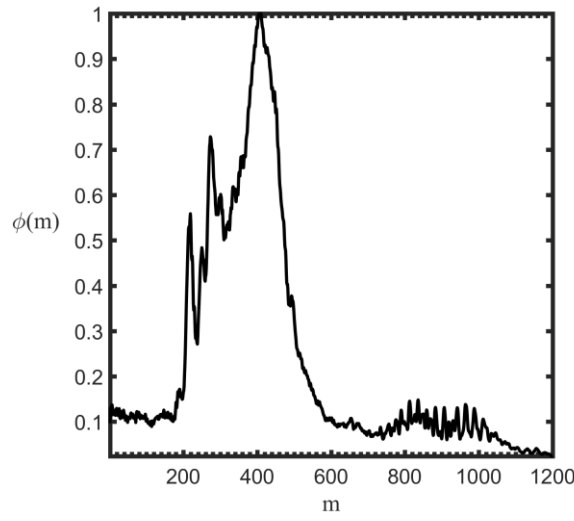


Figure 7. Averaging poloidal spectrum.

Electrostatic potential ϕ on diagnosis flux surface is given in FIG8. X axis is ζ , changing from 0 to 2π , and y axis is θ , changing from $-\pi$ to π . It shows 5 up-and-down clusters in (ζ, θ) space. 3D mode structure of electrostatic potential on diagnosis flux surface is given in FIG9. They show the discrete toroidal symmetry of W7-X and reflect 5 field periods' effects. The mode structures repeat after rotating one field period, but still exit difference on potential intensity.

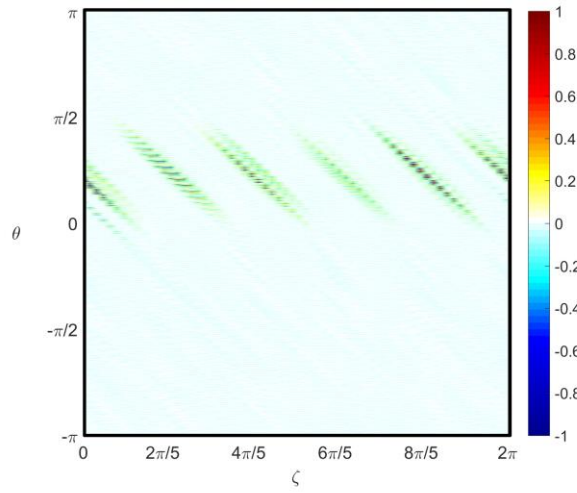


Figure 8. Phi on flux surface when keeping all nmodes. X axis is ζ and y axis is θ .

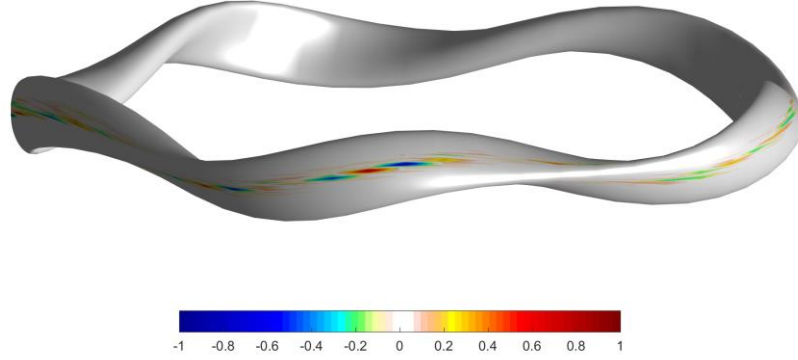


Figure 9. 3D electrostatic potential mode structure of W7-X.

IV. SIMULATION OF ITG IN LHD

For LHD, device configuration is different from that of W7-X. In LHD, field period N_{fp} is 10, and

2D poloidal contours at $\zeta = \frac{0}{N_{fp}}, \frac{0.5\pi}{N_{fp}}, \frac{\pi}{N_{fp}}, \frac{1.5\pi}{N_{fp}}$ on diagnosis flux surface are given in

FIG10. Ion temperature and rotational transform profiles used in simulation of LHD are presented in FIG11(a), and simulation range of ψ is marked out and diagnosis point is at $\psi=0.375$. Basic parameters are as follows: magnetic field on axis is 14457.83 Gauss, ion temperature on axis is 1000 eV, major radius is 372.8 cm, $k_{\perp}\rho_i=0.0098$, time step is 0.004 Cs/R0, and Cs/R0 is 5.98E-04. Growth rates and real frequencies are normalized to Cs/R0 in this section. Fourier series coefficients in ζ expansion are also used in LHD, like the method to build magnetic field of W7-X.

The first 4 Fourier series coefficients profiles $B_{cn}(\psi,1,1)$, $B_{cn}(\psi,1,2)$, $B_{cn}(\psi,1,3)$,

$B_{cn}(\psi,1,4)$ used to construct 3D magnetic field of LHD are given in FIG11(b), and in LHD,

Fourier series $ntor(n)$ is an arithmetic progression with common difference of 10 due to its field period, and the first 4 harmonic Fourier series $ntor(n)$ are 0, 10, 20, 30.

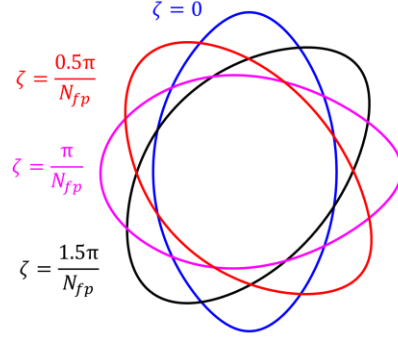


Figure 10. 2D poloidal contours of LHD on diagnosis flux surface at $\zeta = 0$ (blue), $\zeta = 0.5\pi / N_{fp}$ (red), $\zeta = \pi / N_{fp}$ (magenta) and $\zeta = 1.5\pi / N_{fp}$ (black). $N_{fp} = 10$ in LHD.

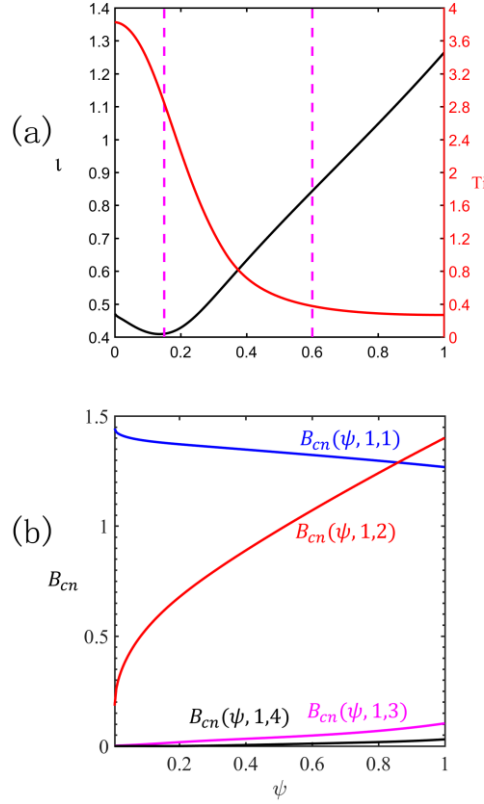


Figure 11. (a) Ion temperature (red) and rotational transform (blue) profiles. Simulation range is marked out by magenta lines: $\psi_{inner}=0.15$ and $\psi_{outer}=0.6$. (b) Fourier series coefficients to build magnetic field of LHD in GTC, $B_{cn}(\psi, 1, 1)=0$ (blue), $B_{cn}(\psi, 1, 2)=5$ (red), $B_{cn}(\psi, 1, 3)=10$ (magenta), $B_{cn}(\psi, 1, 4)=15$ (black). Values of $B_{cn}(\psi, 1, 2)$ and $B_{cn}(\psi, 1, 3)$ are multiplied by 5. Values of $B_{cn}(\psi, 1, 4)$ are multiplied by 20.

Considering field period of LHD is 10, more parallel grids are needed in simulations of LHD than W7-X. Parallel grids are set as 81, 121, 161, and growth rates and real frequencies of $n_{mode}=37$, $m_{mode}=61$ are given in FIG12. For LHD, 121 grids in parallel direction are necessary to get convergence in full torus simulations of LHD. According to parallel grids convergence of W7-X

and LHD, 12 or more toroidal grids are needed for every field period of stellarators using GTC. Influences of modes coupling on growth rates and real frequencies in LHD are also studied. Applying the same analysis method like in W7-X, one nmode, 3 nmodes, 7 nmodes and all nmodes are kept in four cases by adding a filtering step. For one nmode case, nmode=37 is kept. For Nmode=3, nmodes=27, 37, 47 are kept, and for Nmode=7, nmodes=7, 17, 27, 37, 47, 57, 67 are kept. Growth rates and real frequencies of nmode=37, mmode=61 are calculated and presented in FIG13. Results show that growth rates and real frequencies of different nmodes coupling does not differ a lot in LHD, and the maximum value and the minimum value differs about 4%.

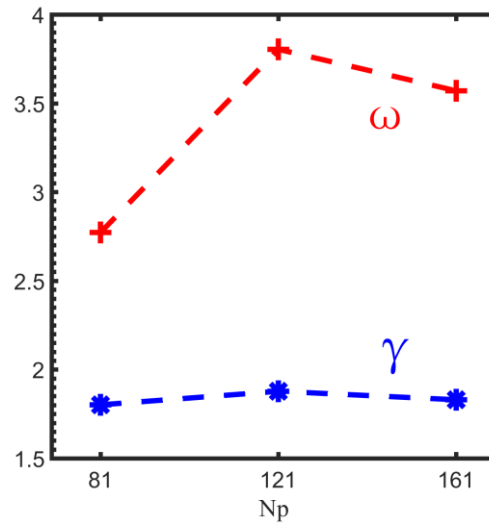


Figure 12. Growth rates (blue) and real frequencies (red) of parallel grids convergence.

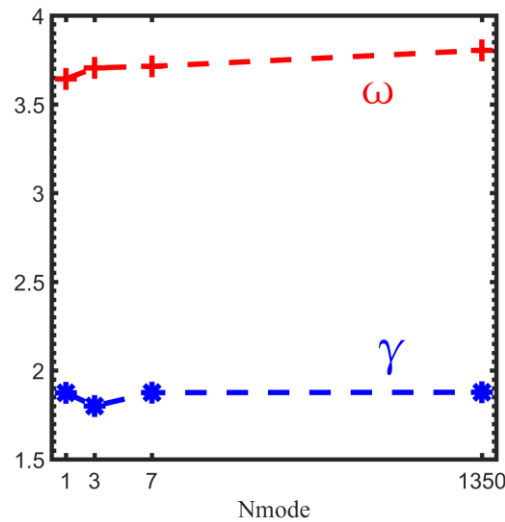


Figure 13. Growth rates (blue) and real frequencies (red) of Nmode convergence.

To study the most unstable modes in LHD, an average poloidal spectrum of diagnosis flux surface and other 10 flux surfaces, which are closest to diagnosis flux surface, is given in FIG14. The most unstable mode is around mmode=64 in LHD, and compared with W7-X, it is lower.

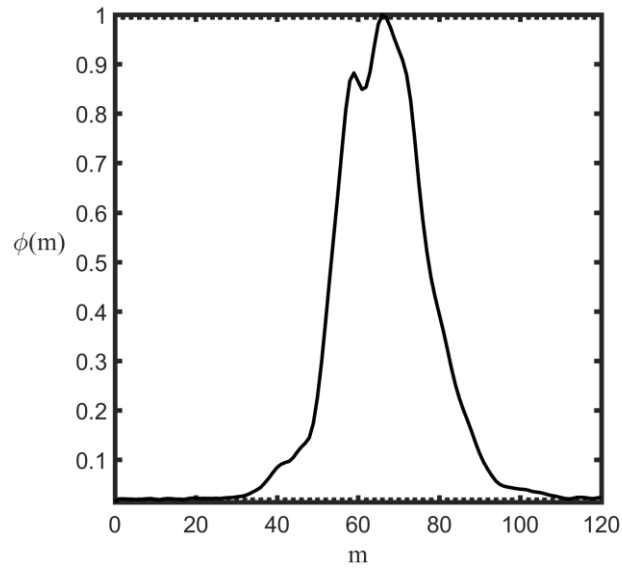


Figure 14. Averaging poloidal spectrum of different flux surfaces. X axis is mmode.

Electrostatic potential ϕ on diagnosis flux surface is shown in FIG15. 3D structure of electrostatic potential on diagnosis flux surface is shown in FIG16, along with device configuration of LHD. The potential intensity shows big difference between field periods, which is similar to W7-X, but is more obvious.

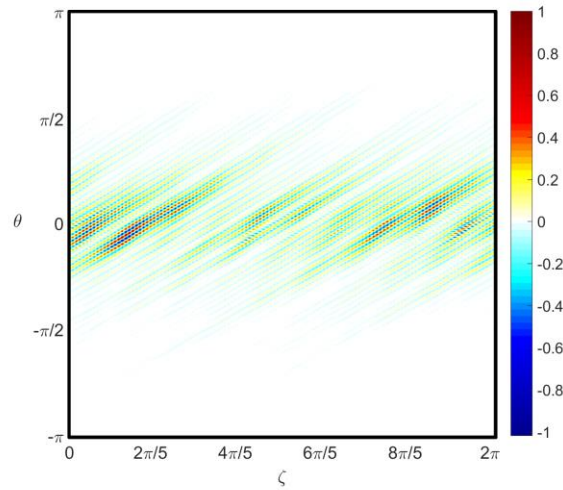


Figure 15. Phi on diagnosis flux surface. X axis is ζ , from 0 to 2π , and y axis is θ , from $-\pi$ to π .

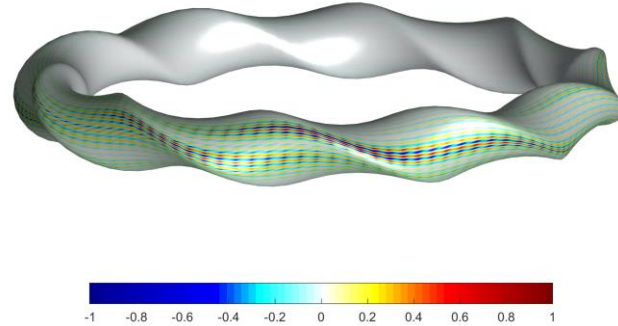


Figure 16. 3D electrostatic potential mode structure of LHD.

V. CONCLUSION AND DISCUSSION

GTC is developed to study plasma behaviors in non-axisymmetric equilibrium configuration. Simulation results of ITG driven instabilities in W7-X and LHD using GTC are given in Section III and Section IV. Linear relation of growth rates and real frequencies of ion temperature gradient in W7-X is studied and compared with results of EUTERPE. Toroidal grids convergence of stellarators helps better understating feature of stellarators and helps future works in stellarators using GTC. Different nmodes coupling in W7-X and LHD is also studied in this article. Due to simulation results, the mode structure in W7-X is more localized, and LHD is more global and tokamak-like. The most unstable modes driven by ITG in W7-X and LHD are different, and it is higher in W7-X. The mode structure effected by mode coupling is more serious in LHD than W7-X. Future works on stellarators using GTC will be focusing on Alfven eigenmodes, like toroidal Alfven eigenmode.

Reference

- 1.Jr, Lyman Spitzer. "The Stellarator Concept." IEEE Transactions on Plasma Science 9.4(1958):130-141.
- 2.Spong, Don. "3D toroidal physics: testing the boundaries of symmetry breaking." Physics of Plasmas 22.5(2015):055602.
- 3.Helander, P, et al. "Stellarator and tokamak plasmas: a comparison." Plasma Physics & Controlled Fusion 54.12(2012):124009.
- 4.Kornilov, V., et al. "Gyrokinetic global three-dimensional simulations of linear ion-temperature-gradient modes in Wendelstein 7-X." Physics of Plasmas 11.6(2004):3196-3202.
- 5.Riemann, J., R. Kleiber, and M. Borchardt. "Effects of radial electric fields on linear ITG instabilities in W7-X and LHD." 58.7(2016):074001.
- 6.Xanthopoulos, P, et al. "Nonlinear gyrokinetic simulations of ion-temperature-gradient

- turbulence for the optimized Wendelstein 7-X stellarator. " Physical Review Letters 99.3(2007).
- 7.Helander, P, et al. "Advances in stellarator gyrokinetics." Nuclear Fusion55.5(2015):053030.
- 8.Ferrandomargalet, S., H. Sugama, and T. Watanabe. "Zonal flows and ion temperature gradient instabilities in multiple-helicity magnetic fields." Physics of Plasmas 14.12 (2007).
- 9.Nunami, M., T. H. Watanabe, and H. Sugama. "THC/P4-20 Effects of Three-Dimensional Geometry and Collisions on Zonal Flows and Ion Temperature Gradient Modes in Helical Systems." (2010).
- 10.Lin Z, et al. "Turbulent transport reduction by zonal flows: massively parallel simulations." Science 281.5384(1998):1835.
- 11.Hirshman, S. P., and J. C. Whitson. "Steepest - descent moment method for three - dimensional magnetohydrodynamic equilibria." 26.12(1983):3553-3568.